

Effects of the Complexation by the Mg^{2+} Cation on the Stereochemistry of the Sugar–Diphosphate Linkage. Ab Initio Modeling on Nucleotide–Sugars

Isabelle André, Igor Tvaroska,* and Jeremy P. Carver

GlycoDesign Inc., 480 University Avenue, Suite 900, Toronto, Ontario, Canada M5G 1V2

Received: January 5, 2000; In Final Form: March 17, 2000

Ab initio molecular orbital calculations of the 2-*O*-methyl-diphosphono-tetrahydropyran dianion (**1**) and the complex of magnesium with 2-*O*-methyl-diphosphono-tetrahydropyran (**2**) are used to model the conformational behavior of the sugar–diphosphate linkage in sugar–nucleotides. The geometry and energy of each conformer were calculated at different basis set levels, from 6-31G* to cc-pVTZ(-f)++, using the SCF, DFT/B3LYP, and LMP2 methods. The vibrational frequencies were calculated at the HF/6-31G* level and the zero-point energy, thermal, and entropy corrections were evaluated. The results of conformational analyses of **1** and **2** clearly show that interactions of the diphosphate linkage with the Mg^{2+} cation alter the conformational preferences about the anomeric and the diphosphate linkages. These changes influence the overall 3D shape adopted by nucleotide–sugars and, therefore, might have consequences for their functions in biological processes. The effects of solvation and of the full first hydration shell of the metal on the stability of relevant conformers have also been calculated. The results show that a delicate balance between intramolecular and intermolecular interactions determines the conformational equilibrium around the sugar–diphosphate linkage. As a result, the sugar–diphosphate linkage can adopt several different conformations depending on the environment.

1. Introduction

The diphosphate functional group occurs in a variety of biological molecules and has an important role in many biological reactions. In nucleotide–sugars, for example, the diphosphate group links a sugar residue with a nucleoside. It is well-known that nucleotide–sugars are involved in the biosynthesis of the saccharide part of glycoconjugates. Glycosyltransferases transfer a sugar from sugar-donor substrates, most commonly nucleotide-diphosphate-sugars, to a specific sugar-acceptor and together with glycosylhydrolases they are involved in the synthesis of complex carbohydrates.¹ Several oligosaccharide structures formed by these reactions constitute important binding determinants involved in biological processes related to cancer.² The pyrophosphate group of nucleotide–sugars acts as the leaving group in the transfer of a sugar residue to an acceptor-molecule. It is also thought that the bond cleaved in the sugar–phosphate linkage is activated by complexation with a divalent cation. Despite the importance of nucleotide–sugars in the catalytic mechanism of glycosyltransferases, their structural behavior has not yet been well understood. The conformation adopted by the sugar–diphosphate linkage largely determines the 3-D structure of nucleotide–sugars. Therefore, the characterization of this linkage is a prerequisite to a deeper understanding of nucleotide–sugar properties. Recently, as a first step in this direction, we have performed the ab initio conformational analyses of the sugar–monophosphate linkage³ and the diphosphate linkage⁴ using the 2-*O*-methylphosphono-tetrahydropyran anion, sodium 2-*O*-methylphosphono-tetrahydropyran, the dimethyl diphosphate dianion, and magnesium dimethyl diphosphate as models. The results revealed an unusual conformational preference around the C1–O1 bond in the 2-*O*-

methylphosphono-tetrahydropyran anion that has been termed the reverse exo-anomeric effect. Interactions with the sodium counterion completely modified these conformational features. Similarly, results on the dimethyl diphosphate dianion and the magnesium dimethyl diphosphate showed considerable effects on the structure and relative energy of the conformers when the metal cation was present. As a continuation of these studies, we present here an extensive investigation of the structural and conformational behavior of the sugar–diphosphate linkage including the effects of interactions with the Mg^{2+} divalent cation. The influence of the first coordination sphere of the Mg^{2+} cation on the conformational properties of the complex will also be explored. The results of this investigation provide information on the conformational equilibrium around the sugar–diphosphate linkage that should be crucial for the design of glycosyltransferase inhibitors.⁵ Moreover, these results could be used as benchmarks for the parametrization and testing of molecular force fields for molecules containing this segment of atoms.

2. Models and Computational Procedures

The conformational behavior of the diphosphate functional group linked to the anomeric carbon in hexopyranosides has been studied by ab initio methods using the 2-*O*-methyl-diphosphono-tetrahydropyran dianion (**1**) and the magnesium 2-*O*-methyl-diphosphono-tetrahydropyran complex (**2**) as models. Structures of the compounds with axially oriented diphosphate groups are illustrated in Figure 1 together with UDP-GlcNAc [uridine 5'-(2-acetamido-2-deoxy- α -D-glucopyranosyl pyrophosphate)] representing the nucleotide-diphosphate-sugars. For a description of the atoms (Figure 1) we have used the atom numbering as in the carbohydrate nomenclature, where the anomeric carbon is denoted as C1, etc. By analogy with the glycosidic linkage of oligosaccharides, we will use the term “sugar–phosphate linkage” for the C1–O1–P3 bonds. Two

* Corresponding author. On leave of absence from the Institute of Chemistry, Slovak Academy of Sciences, Bratislava, Slovak Republic.

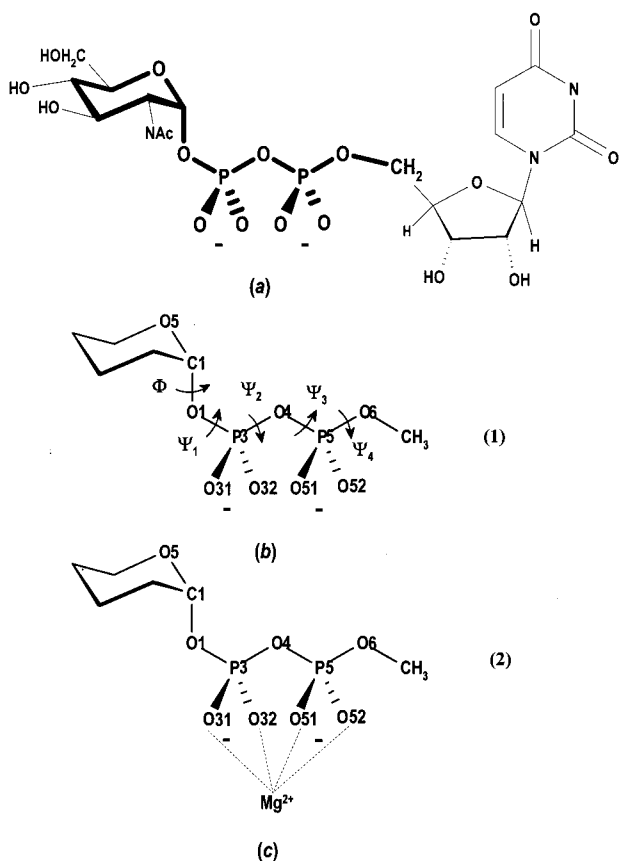


Figure 1. Schematic representation of (a) uridine diphosphate-*N*-acetylglucosamine (the highlighted part has been modeled in this work), (b) 2-*O*-methyldiphosphono-tetrahydropyran dianion (**1**) and (c) magnesium 2-*O*-methyldiphosphono-tetrahydropyran complex (**2**).

dihedral angles define the conformation around this linkage. The rotation about the anomeric C1–O1 linkage is described by the dihedral angle Φ [$\Phi = \Phi(\text{O5} - \text{C1} - \text{O1} - \text{P3})$], and the orientation about the O1–P3 bond, by the dihedral angle Ψ_1 [$\Psi_1 = \Psi_1(\text{C1} - \text{O1} - \text{P3} - \text{O4})$]. Orientations of the diphosphate group are described by two dihedral angles Ψ_2 [$\Psi_2 = \Psi_2(\text{O1} - \text{P3} - \text{O4} - \text{P5})$] and Ψ_3 [$\Psi_3 = \Psi_3(\text{P3} - \text{O4} - \text{P5} - \text{O6})$]. Finally, the dihedral angle Ψ_4 [$\Psi_4 = \Psi_4(\text{O4} - \text{P5} - \text{O6} - \text{C})$] describes the orientation of the terminal methyl group which in this case models the methylene group of the nucleoside part of sugar–nucleotides. The conformation of compounds **1** and **2** is then described using five torsion angles Φ , Ψ_1 , Ψ_2 , Ψ_3 , and Ψ_4 . Three staggered orientations about the C1–O1 and P–O bonds are denoted as G (synclinal, gauche, 60°), T (antiperiplanar, trans, 180°), and mG (–synclinal, –gauche, –60°), respectively. The eclipsed orientations about these bonds are denoted as C (synperiplanar, cis, ~0°), A (antiperiplanar, ~120°), and mA (–antiperiplanar, ~–120°), respectively. In this notation, e.g., AGTmGmA means that the angles Φ , Ψ_1 , Ψ_2 , Ψ_3 , and Ψ_4 are approximately in the antiperiplanar (ap), synclinal (sc), or gauche (G), antiperiplanar (ap) or trans (T), –synclinal (–sc), or –gauche (mG), and –antiperiplanar (–ap, mA) conformation, respectively.

The ab initio calculations were carried out with the Turbomole 95.0⁶ and GAMESS⁷ programs using standard basis sets. The optimization of the geometry was performed at the SCF level with the 6-31G* basis set. The geometry was fully optimized using the gradient optimization routines of the program without any symmetry constraints. For several relevant minima of **1** and **2**, more extensive calculations using different methods and different basis sets were performed using the Jaguar program.⁸

The vibrational frequencies were calculated at the HF/6-31G* level and the zero-point energy, thermal, and entropy corrections were evaluated. The relevant conformers were also calculated using a hybrid Hartree–Fock–density functional scheme, the adiabatic connection method B3LYP⁹ of density functional theory¹⁰ (DFT). We utilized the standard 6-31G** and 6-31++G** basis sets for the geometry optimization. Single point calculations were carried out with the cc-pVTZ(-f)++ basis set for **1**. Local MP2 calculations¹¹ (LMP2) were then performed on these geometries with the cc-pVTZ(-f)++ basis set for **1** and with the 6-31++G** basis set for **2**. The electron correlation effects were treated by means of DFT/B3LYP and LMP2. The solvent effects on the conformational equilibrium have been investigated with a self-consistent reaction field method¹² as implemented in Jaguar at the DFT/B3LYP/6-31G** level, using the Poisson–Boltzmann solver and including empirical corrections to repair deficiencies in both the ab initio and continuum solvation models. Solvation calculations were carried out for two solvents, namely cyclohexane ($\epsilon = 2.023$) and water ($\epsilon = 80.37$) using the geometries calculated in the gas phase.

3. Results and Discussion

A. 2-*O*-Methyldiphosphono-tetrahydropyran Dianion (**1**).

The conformation of the sugar–diphosphate and diphosphate linkages in the 2-*O*-methyldiphosphono-tetrahydropyran dianion (**1**) is described by five internal rotational degrees of freedom associated with the C1–O1, O1–P3, P3–O4, O4–P5, and P5–O6 bonds (Figure 1b). The assumption of three staggered conformers for each bond would generate 243 (3⁵) conformers to be considered. Therefore, a systematic grid search using high-level ab initio calculations of these conformers would require excessive computer time. We utilized then the results on structurally related models, the 2-*O*-methylphosphono-tetrahydropyran anion⁴ and the dimethyl diphosphate dianion,³ as a guide to restrict the conformational space of **1**. The study of the 2-*O*-methylphosphono-tetrahydropyran anion gave important information on the preferred orientations observed about the sugar–phosphate linkage (Φ , Ψ_1 dihedral angles), whereas the study of both the 2-*O*-methylphosphono-tetrahydropyran anion and the dimethyl diphosphate dianion provided data on the more favorable conformation of the diphosphate linkages (Ψ_2 and Ψ_3 dihedral angles). The combination of all this information significantly reduced the number of conformers by generating only 100 starting structures for geometry optimization. Three staggered conformations around the C1–O1 bond had been calculated for the 2-*O*-methylphosphono-tetrahydropyran anion, namely, the sc, ap, and –sc orientations. Conformers adopting the –sc orientation about the C1–O1 bond had a higher relative energy (6.7–9.4 kcal/mol) due to the presence of unfavorable steric interactions of the phosphate group with the pyranoid ring atoms. We presumed that such interactions might be more severe for the larger diphosphate group. Indeed, preliminary calculations of several conformers with the –sc orientation showed that the optimization changed the orientation around the C1–O1 bond from the –sc to the ap conformation. Therefore, during the generation of the starting conformations of **1**, the –sc orientation for the Φ dihedral angle has not been considered. The calculated relative energies and dihedral angles of the final HF/6-31G* minima are gathered in Table 1.

As can be seen from Table 1, the optimization of the 100 starting structures at the HF/6-31G* level led to 37 distinct minima. The energies of all minima cover a relatively small interval of 8.5 kcal/mol. This suggests that the sugar–diphos-

TABLE 1: Ab Initio Relative Energy (kcal/mol), and Position of Conformational Minima of the 2-*O*-Methyldiphosphono-tetrahydropyran Dianion (1) Calculated at the HF/6-31G* Level

conformer	Φ	Ψ_1	Ψ_2	Ψ_3	Ψ_4	ΔE
AAmGmAG	104.1	107.7	-59.9	-101.8	73.3	0.00 ^a
AGGAmG	153.5	83.9	63.7	93.1	-76.8	0.73
AAGGG	135.4	91.3	46.8	18.3	75.6	1.24
AAmGmGmG	108.9	101.6	-45.2	-38.5	-70.5	1.28
TmGAGmG	173.3	-55.8	90.8	74.1	-87.1	1.77
AAmGAmG	97.2	110.3	-60.1	135.6	-66.2	2.25
TAmAmGmG	162.6	91.9	-134.4	-47.5	-62.7	2.61
TGTmAG	162.4	89.1	-150.4	72.6	-92.7	2.69
TGTmAG	159.5	83.3	-172.4	-111.2	70.5	2.76
GmAmGmGG	88.4	-92.2	-69.8	-74.1	88.7	2.80
TmGAGG	176.5	-55.6	90.0	54.8	53.8	3.02
TmGmGmGG	-176.3	-34.5	-71.5	-67.2	87.2	3.28
TmGmGCmG	-175.8	-44.8	-57.0	-27.2	-71.7	3.39
TmGGmAG	159.2	-89.3	72.5	-133.4	68.1	3.47
AmAmGmGmG	90.2	-108.1	-59.1	-46.7	-62.8	3.50
AAmATG	137.6	94.6	-111.4	-177.7	66.3	3.58
GTGAmG	72.1	158.7	58.4	96.9	-78.4	3.79
TmGAAT	173.6	-54.5	100.5	100.5	-169.7	3.97
TmGATmG	173.9	-54.9	99.7	-168.5	-66.7	3.98
AmAGGG	103.6	-136.6	35.1	47.0	64.0	4.18
TmGTAmG	156.9	-59.9	-175.9	103.7	-73.9	4.52
AAmGAT	98.8	106.6	-48.9	108.4	179.1	4.63
AmAmGTmG	100.7	-91.5	-70.9	163.9	-68.9	5.04
TAGTG	157.2	106.3	63.5	179.9	64.5	5.04
TTAmGA	173.5	-153.5	100.1	-42.6	95.2	5.34
GmATmAG	73.8	-92.7	157.4	-91.7	77.2	5.57
TGGmAT	150.8	85.7	69.4	-143.4	-179.5	5.59
GTGmAG	69.4	159.4	58.8	-132.5	68.0	5.75
TmGmAGG	151.2	-65.0	-120.4	59.0	65.0	5.96
GmATmGmG	73.5	-90.8	163.7	-46.4	-64.0	6.11
TTGG	173.3	-152.0	167.0	33.2	71.7	6.27
TmAAmGmG	174.4	-149.2	103.2	-50.3	-71.7	6.28
TmGATT	175.3	-57.8	95.0	-161.2	-180.0	6.50
GATGG	75.4	142.2	158.7	35.8	68.9	6.74
TATAG	161.4	97.4	-176.2	99.4	82.8	7.14
GmAmGTT	89.5	-91.0	-71.5	151.9	177.2	7.82
TmGmGAT	-174.8	-33.7	-68.9	145.0	-178.3	8.50

^a $E = -950\,507.26$ kcal/mol.

phate linkage in **1** is quite flexible but that this flexibility is restricted to a small part of the potential energy hypersurface. Analysis of the results also indicates that transitions between different conformers about the O1–P4–O5–P5–O6 bond sequence require a concerted rotation about at least two bonds with the sole exception of the Ψ_4 dihedral angle, which describes the free rotation of the external methyl group. Results of the present study show, as for the 2-*O*-methylphosphono-tetrahydropyran anion, an unusual conformational behavior of the sugar–diphosphate linkage. The diphosphate group linked to the anomeric carbon prefers the anticlinal ($\sim 120^\circ$, ac) over the synclinal orientation about the anomeric C1–O1 bond. Such a preference for the ac conformer about the C1–O1 bond observed in sugar–phosphate linkages is unique among the conformations of glycosyl compounds¹³ and this phenomenon has been named the *reverse exo-anomeric effect*.⁴ The anticlinal conformers around the C1–O1 bond can be divided into two groups. The first and more frequent corresponds to the so-called trans conformation ($\Phi \sim 150^\circ$) observed in α -glycosyl compounds.⁴ The second and less frequent group ($\Phi \sim 100^\circ$) represents a unique conformation for the anomeric bond. The four lowest energy conformations (AAmGmAG, AGGAmG, AAGGG, and AAmGmGmG) show the same orientation around the C1–O1 bond with $\Phi \sim 104$ – 154° (ac) and around the O1–P3 bond with $\Psi_1 \sim 83$ – 108° (sc, ac) (Figure 2). These four lowest energy conformers exhibit a clear deviation from the ideal gauche position (sc, 60°) and their relative energies are

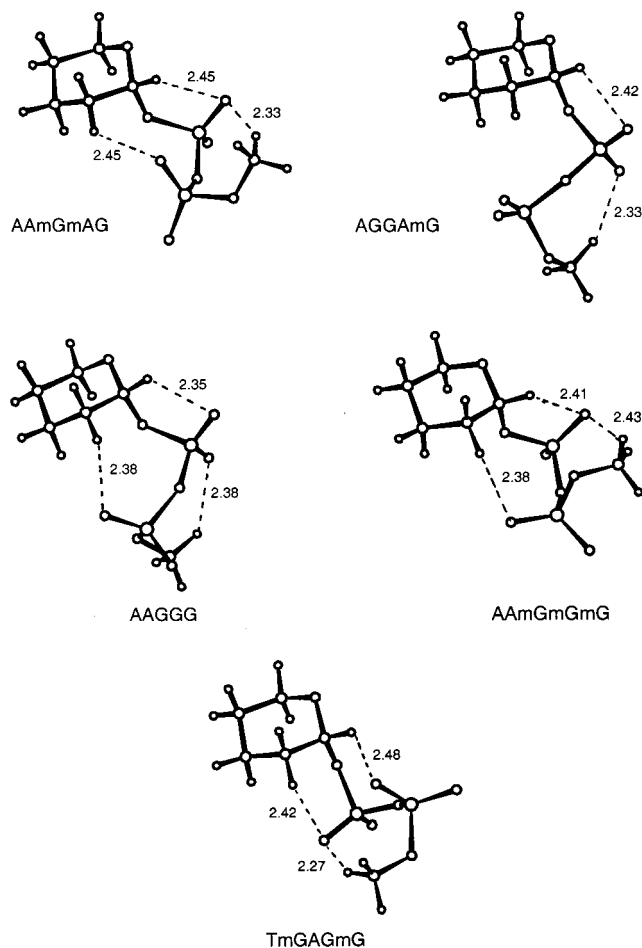


Figure 2. Representation of the hydrogen-bonding patterns observed for the five lowest energy conformers of the 2-*O*-methyldiphosphono-tetrahydropyran dianion (**1**) calculated at HF/6-31G* level. Dashed lines show the CH...O hydrogen-bonding interactions. Bond lengths are given in angstroms.

very close, within 1.3 kcal/mol. From Table 1, it is clear that the sc orientation around the C1–O1 bond is not favored. Indeed, it appears that from 37 final minima, only seven of them adopted the gauche conformation about the C1–O1 bond. The lowest energy conformer (GmAmGmGG) with the sc orientation is 2.8 kcal/mol above the AAmGmAG conformer, which is the lowest energy conformer for the ac orientation.

Previous high-level ab initio calculations performed on monophosphate derivatives have shown a clear preference of the P–O bonds in the C–O–P–O–C bond sequence for the sc conformation. For diphosphate linkages, results have shown a similar dominance of the sc orientation for the P–O bonds in the O–P–O–P–O bond sequence. As can be seen in Table 1, only a few conformers adopted the ap orientation around the P–O bond. This conformation appears to be considerably less stable than the sc orientation. In general, phosphate derivatives in their anionic forms exhibit a strong preference for the sc over the ap conformation around the P–O bond, in accordance with the general anomeric effect. However, in contrast with the results on the dimethyl diphosphate dianion, one of the P–O bonds in **1** is usually shifted from the sc to the ac conformation. The (sc, ac) or (–sc, –ac) arrangements of the O1–P3–O4–P5–O6 segment are present in the two lowest energy conformers (AAmGmAG and AGGAmG) with $(\Psi_2, \Psi_3) = (-60^\circ, -102^\circ)$ and $(64^\circ, 93^\circ)$, respectively. The next two conformations (AAGGG and AAmGmGmG) present another conformation around the P–O–P segment, namely, the sc, sc and –sc, –sc.

TABLE 2: Comparison of the ab Initio Relative Energies (kcal/mol) of Selected 2-O-Methyldiphospho-tetrahydropyran Dianion (1) Conformers Calculated by Different Methods

	method		conformer				
	energy	geometry	AAMGmAG	AGGAmG	AAGGG	AAMGmGmG	TmGAGmG
HF	6-31G*	6-31G*	0.00	0.73	1.24	1.28	1.77
HF	6-31++G**	6-31G*	0.00	0.54	0.29	0.36	1.90
HF	cc-pVTZ(-f)++	6-31G*	0.00	0.54	0.43	1.00	1.88
HF	6-31++G**	6-31++G**	0.00	0.51	0.51	1.34	2.00
HF	cc-pVTZ(-f)++	6-31++G**	0.00	0.32	0.41	1.11	1.90
DFT/B3LYP	6-31G**	6-31G**	0.00	0.67	0.86	0.70	1.26
DFT/B3LYP	6-31++G**	6-31G**	0.00	0.73	0.64	0.49	1.67
DFT/B3LYP	cc-pVTZ(-f)++	6-31G**	0.00	0.65	0.49	0.59	1.83
DFT/B3LYP	6-31++G**	6-31++G**	0.00	0.73	0.64	0.49	1.67
DFT/B3LYP	cc-pVTZ(-f)++	6-31++G**	0.00	0.51	0.44	0.77	1.67
LMP2	cc-pVTZ(-f)++	6-31G*	0.30	0.00	0.08	0.52	1.51
LMP2	cc-pVTZ(-f)++	6-31++G**	0.14	0.00	0.36	0.68	1.75

The corresponding values of dihedral angles are (47° , 18°) and (-45° , -39°), respectively. All these arrangements correspond to conformations observed for the dimethyl diphosphate dianion.³ On the basis of the relative energy of these conformers, we assume the potential energy surface about the Ψ_2 , Ψ_3 dihedral angles to be very flat. Thus, interactions with the environment (protein, counterion, or solvent) can change the conformational preferences around these linkages quite significantly.

Inspection of the three-dimensional structure of the lowest energy conformations of **1** reveals the presence of stabilizing interactions between phosphate oxygen atoms and one of the hydrogens attached to a carbon atom, i.e., C–H...O hydrogen-bonding interactions. Among the low-energy conformers, distinct hydrogen-bonding patterns are observed. These patterns are closely related to the conformation observed around the sugar–phosphate linkage (Φ and Ψ_1 dihedral angles). For instance, the four lowest energy conformers (AAMGmAG, AGGAmG, AAGGG, and AAMGmGmG) with the (ac, ac) orientation around the sugar–phosphate linkage, display similar hydrogen-bonding patterns. As can be seen in Figure 2, where selected conformers are shown, three CH...O interactions involving charged phosphoryl oxygen atoms of both phosphate groups with several hydrogens are usually present in this group of conformers. The relevant geometrical parameters for the different interactions displayed in Figure 2 are C1–H1...O–P3 ($d_{\text{H...O}} \sim 2.4 \text{ \AA}$, $\theta_{\text{C–H...O}} \sim 100\text{--}110^\circ$), CH3...O–P3 ($d_{\text{H...O}} \sim 2.3\text{--}2.4 \text{ \AA}$, $\theta_{\text{C–H...O}} \sim 130\text{--}155^\circ$), and C2–H2...O–P5 ($d_{\text{H...O}} \sim 2.3\text{--}2.4 \text{ \AA}$, $\theta_{\text{C–H...O}} \sim 130\text{--}150^\circ$). The lowest energy conformer with the ap conformation around the C1–O1 linkage, TmGAGmG, displays a distinct hydrogen-bonding motif (Figure 2). Three CH...O interactions are again found, though they involve different atoms. The geometrical parameters characterizing the interactions shown in Figure 2 are C1–H1...O–P5 ($d_{\text{H...O}} \sim 2.5 \text{ \AA}$, $\theta_{\text{C–H...O}} \sim 125^\circ$), CH3...O–P3 ($d_{\text{H...O}} \sim 2.3\text{--}2.4 \text{ \AA}$, $\theta_{\text{C–H...O}} \sim 147^\circ$) and C2–H2...O–P3 ($d_{\text{H...O}} \sim 2.3\text{--}2.4 \text{ \AA}$, $\theta_{\text{C–H...O}} \sim 120^\circ$). The geometrical parameters observed are characteristic of CH...O hydrogen-bonding interactions described in the literature.^{14,15} The comparison of both patterns observed reveals very similar short (C–)H...O contacts, but different phosphoryl oxygen atoms are involved in each case. These patterns can almost be considered as inverted. Clearly, the different conformations of the pyrophosphate group are stabilized by such interactions.

To clarify the importance of these interactions in the stabilization of anionic phosphate derivatives, we have compared these patterns with similar structural features observed in the dimethyl diphosphate dianion. The dimethyl diphosphate dianion is a symmetric molecule terminated by methyl groups at both

extremities and the conformation of this molecule is then not influenced by the presence of a sugar unit. The main factor controlling the overall conformation of such a molecule is the flexibility around the P–O–P segment. For the dimethyl diphosphate dianion, the preferred arrangement for the O–P–O–P–O bond segment (Ψ_2 and Ψ_3 dihedral angles) is (sc, sc) or its symmetrically related (–sc, –sc). Despite a slight shift from the ideal “staggered” position, the dimethyl diphosphate dianion exhibits a similar preference for the synclinal conformation around the phosphate linkage as well as almost identical intramolecular hydrogen-bond patterns. Both phosphate groups are stabilized by CH...O(–P) interactions involving the two external methyl groups.³ For instance, the lowest energy conformers (mGGGmG and GGGG) of the dimethyl diphosphate dianion show the presence of two symmetrical short contacts ($d_{\text{H...O}} = 2.3$ and 2.4 \AA , respectively) involving each of the phosphate groups with the farthest methyl group. Obviously, the occurrence of C–H...O(–P) interactions in these structures is not fortuitous and it definitely points out the role they may have in the stabilization of phosphate derivatives. Such long-range hydrogen-bonding interactions have often shown their great importance in crystal engineering.^{15,16}

Recent calculations on carbohydrate model compounds¹³ and dimethyl diphosphate¹⁷ suggested that calculations with the 6-31G* basis sets at the HF level provide a reasonable set of conformational energies and geometries. Our recent calculations on the sugar–monophosphate linkage³ and the diphosphate linkage⁴ also support this suggestion. On the other hand, because a dianion is involved in the system investigated, the inclusion of diffuse functions should give more reliable results.¹⁸ Therefore, to test the reliability of the results calculated at the HF/6-31-G* (272 basis functions) level, we have run a series of calculations on five representative conformers, namely AAMGmAG, AGGAmG, AAGGG, AAMGmGmG, and TmGAGmG, at the HF/6-31++G** (384 basis functions), HF/cc-pVTZ(-f)++ (676 basis functions), and LMP2/cc-pVTZ(-f)++ levels. Density functional theory based on adiabatic connection arguments, which incorporates an admixture of Hartree–Fock exchange in a linear combination with the usual density functional ingredients,⁹ have been shown to provide good quality geometries. We also utilized the DFT/B3LYP/6-31G** (308 basis functions) and the DFT/B3LYP/6-31++G** levels for geometry optimization and the DFT/B3LYP/cc-pVTZ(-f)++ level for single point calculations of the energy. The results of these calculations are gathered in the Tables 2 and 3.

The selected geometrical parameters for five conformers of **1** are listed in Table S1 of the Supporting Information. The results show that the change in geometry when going from the

TABLE 3: Summary of the Corrections to the Calculated Free Energy Differences (ZPE, ΔG_{vibrot} , $\Delta G(\text{cyclohexane})_{\text{Solv}}$, $\Delta G(\text{water})_{\text{Solv}}$, Energies (ΔE), and Estimated Free Energies (ΔG_{gas} , $\Delta G_{\text{cyclohexane}}$, ΔG_{water})^a for the AAmGmAG, AGGAmG, AAGGG, AAmGmGmG, and TmGAGmG Conformers of 2-*O*-Methyldiphosphono-tetrahydropyran Dianion (1**) in the Gas Phase, Cyclohexane, and Water at 298 K (kcal/mol)**

	method	AAmGmAG	AGGAmG	AAGGG	AAmGmGmG	TmGAGmG
ZPE	HF/6-31G*	121.28	120.64	122.17	120.86	120.49
ΔG_{vibrot}	HF/6-31G*	-28.20	-28.11	-28.10	-28.18	-27.86
$\Delta G(\text{cyclohexane})_{\text{Solv}}$	DFT/B3LYP/6-31G**	-89.84	-90.05	-88.11	-89.82	-88.57
$\Delta G(\text{water})_{\text{Solv}}$	DFT/B3LYP/6-31G**	-204.14	-205.44	-200.81	-203.71	-202.74
ΔE	HF/cc-pVTZ(-f)++//6-31++G**	0.00	0.32	0.41	1.11	1.90
ΔG_{gas}		0.24	0.00	1.63	0.94	1.04
$\Delta G_{\text{cyclohexane}}$		0.40	0.00	2.09	0.76	1.26
ΔG_{water}		1.49	0.00	4.78	2.16	2.48
ΔE	DFT/B3LYP/cc-pVTZ(-f)++//6-31++G**	0.00	0.51	0.44	0.77	1.67
ΔG_{gas}		0.05	0.00	1.47	0.41	1.25
$\Delta G_{\text{cyclohexane}}$		0.20	0.00	1.94	0.23	1.48
ΔG_{water}		1.30	0.00	4.63	1.73	2.70
ΔE	LMP2/cc-pVTZ(-f)++//6-31++G**	0.14	0.00	0.36	0.68	1.75
ΔG_{gas}		0.69	0.00	1.90	0.84	1.85
$\Delta G_{\text{cyclohexane}}$		0.85	0.00	2.36	0.65	2.07
ΔG_{water}		1.94	0.00	5.05	2.15	3.28

$$^a \Delta G_{\text{gas}} = \Delta E + \text{ZPE} + \Delta G_{\text{vibrot}}; \Delta G_{\text{cyclohexane}} = \Delta G_{\text{gas}} + \Delta G(\text{cyclohexane})_{\text{Solv}}; \Delta G_{\text{water}} = \Delta G_{\text{gas}} + \Delta G(\text{water})_{\text{Solv}}$$

HF/6-31G* level to the HF/6-31++G**, DFT/B3LYP/6-31G** or DFT/B3LYP/6-31++G** levels is rather small. Usually the change in any torsional angle is less than 15°. An exception is, however, the Φ_3 torsional angle of the AAmGmGmG and AGGAmG conformers where larger differences were observed. Differences in the bond angles calculated at all levels of theory are within 5°. Comparison of bond lengths revealed that the trends observed in the geometries at the HF/6-31G* level remain at the HF/6-31++G**, DFT/B3LYP/6-31G** and DFT/B3LYP/6-31++G** levels. It is noteworthy, however, that the HF/6-31G* bonds are systematically shorter than the DFT/B3LYP/6-31G** bonds. For example, the C–O bond is typically shorter by 0.02 Å (1.376–1.398 Å versus 1.398–1.419 Å) and the P–O single bond lengths are typically 0.03–0.04 Å shorter (1.612–1.652 Å versus 1.648–1.703 Å). Such a systematic difference was also noticed in previous calculations³ and is likely a characteristic of the 6-31G* basis set. Further expansion of the basis set by adding diffuse functions does not alter bond lengths. Indeed, the bond lengths observed at HF/6-31G* versus HF/6-31++G** levels and at DFT/B3LYP/6-31G** versus DFT/B3LYP/6-31++G** levels, are roughly the same.

Table 2 presents the relative energies for the seven conformers of **1** calculated at the different levels. A comparison of the relative energies shows that an increase of the basis set decreases energy differences. The HF/6-31G* energies display the largest differences observed (up to 0.9 kcal/mol) compared with the LMP2/cc-pVTZ(-f)++//6-31++G** results. Inclusion of the diffuse functions into the basis set, i.e., 6-31G* versus 6-31++G**, significantly decreases these differences. This is also observed for single point calculations when using the HF/6-31G* geometry. These findings together with the large deviations observed in the Φ_3 dihedral angle of some conformers suggest that the basis sets with diffusion functions are more appropriate than the 6-31G* basis set for accurate prediction of the structure and relative energy of dianionic diphosphate systems. Despite the general agreement, both HF and DFT/B3LYP methods erroneously predict the lowest energy conformer compared to the LMP2 method. The LMP2/cc-pVTZ(-f)++//6-31++G** results show a preference for the AGGAmG conformer over the AAmGmAG by 0.14 kcal/mol. At all levels of HF and DFT/B3LYP calculations, the AAmGmAG is predicted as the lowest energy conformer. This preference increases from 0.3 to 0.7 kcal/mol.

The influence of the solvent on the relative stability of conformers around the C1–O1 bond in carbohydrate derivatives

is well documented.¹⁹ To provide insight into the importance of solvent effects on the stability of the sugar–phosphate linkage conformers, we have calculated the solvation energies for seven selected conformers of **1** using the DFT/B3LYP/6-31G** method and the Jaguar program.⁸ These results together with the calculated zero-point vibrational energies, the thermal energies, and the entropies at the HF/6-31G* level are given in Table 3. These values were combined with the ΔE values calculated at different basis sets in order to give different estimates of ΔG_{gas} , $\Delta G_{\text{cyclohexane}}$, and ΔG_{water} . Examination of the data in Tables 2 and 3 clearly revealed that after considering the thermodynamic corrections, the AGGAmG is the preferred conformer. At the three highest levels of theory used, HF/cc-pVTZ(-f)++//6-31++G**, DFT/B3LYP/cc-pVTZ(-f)++//6-31++G**, and LMP2/cc-pVTZ(-f)++//6-31++G**, the gas phase relative energies are +0.32, +0.51, and -0.14 kcal/mol, respectively. After including the zero-point vibrational energies, thermal energies, and entropies, the calculations predict the relative free energies of the AGGAmG conformer to be -0.24, -0.05, and -0.69 kcal/mol, respectively. As can be seen in Table 3, there is a 2 kcal/mol variation in the predicted solvation energies of the conformers in cyclohexane solution and a 5.5 kcal/mol variation in aqueous solution. Calculated solvation free energies in water (from -200.8 to -205.4 kcal/mol) are in accordance with the value of -195.8 kcal/mol calculated by the polarized continuum model for the pyrophosphate dianion.²⁰ The preference for the AGGAmG conformer is clearly more pronounced in solution than in the gas phase. Both cyclohexane and water stabilize this conformer since, at the highest level of theory, this conformer is preferred by 0.65 kcal/mol in cyclohexane and by 1.94 kcal/mol in water.

B. Magnesium 2-*O*-Methyldiphosphono-tetrahydropyran Complex (2**).** The inclusion of a magnesium cation into molecule **1** introduces new conformational variables such as the possibility of several locations for the Mg^{2+} with respect to the diphosphate group.³ This considerably complicates the conformational analysis of the magnesium 2-*O*-methyldiphosphono-tetrahydropyran complex (**2**) (Figure 1c) compared to **1**. To restrict the complexity of the conformational space to a more manageable dimension, we have used previous results on a related model, the magnesium dimethyl diphosphate complex. The favored conformations of the diphosphate linkage (Ψ_2 and Ψ_3 dihedral angles) and the locations occupied by the magnesium cation in this molecule have been used as templates to generate the starting structures for geometry optimization of **2**.

TABLE 4: Ab Initio Relative Energy (kcal/mol) and the Position of Conformational Minima of the Magnesium 2-*O*-Methyldiphosphono-tetrahydropyran Complex (2) at the HF/6-31G* Level

conformer	Φ	Ψ_1	Ψ_2	Ψ_3	Ψ_4	Mg ²⁺ coordin	ΔE
GmAGmAmG	87.3	-133.7	61.7	-91.9	-75.5	A	0.00 ^a
GmAGTmG	86.4	-131.5	78.1	-178.9	-59.5	B	4.13
GmAGTG	87.1	-132.4	77.9	178.6	55.1	B	4.56
GGmGTG	48.2	64.4	-87.9	178.2	58.3	B	4.92
GGmGTmG	43.7	68.3	-85.6	-177.5	-56.1	B	5.54
GmAGTT	86.7	-132.4	78.0	-179.9	-177.7	B	5.67
GGmGTT	46.1	66.7	-86.6	-177.9	175.1	B	6.36
GmGmATG	78.5	-83.9	-105.3	176.2	48.0	C	9.67
GmGTmAmG	68.9	-79.4	174.5	-96.8	-69.7	D	9.81
AmGmATmG	92.3	-78.7	-97.3	174.1	-53.2	C	9.86
GGTmAmG	66.4	42.5	174.1	-103.2	-79.5	D	10.21
GGmATG	70.0	60.9	-112.0	-178.1	60.7	C	10.31
GGTAG	76.5	41.6	175.5	110.8	81.4	D	10.40
AATmAmG	118.6	100.1	177.3	-103.5	-77.7	D	10.61
AGTmAmG	144.7	86.9	-179.6	-108.9	-82.5	D	10.64
GmGTAG	84.9	-82.6	-179.8	109.7	84.7	D	10.72
AmGmATG	141.9	-70.6	-109.7	179.8	58.8	C	10.93
AATAG	132.8	91.0	179.0	109.8	79.9	D	11.16
GGmATmG	69.1	60.9	-111.3	-176.7	-58.4	C	11.28
GmGmATT	85.3	-85.5	-104.4	177.8	172.2	C	11.31
GGATmG	51.0	40.5	111.0	179.1	-56.2	C	11.37
GmGTmAG	65.6	-86.3	-172.0	-125.6	62.6	D	11.42
ATATmG	108.1	171.4	109.7	-177.8	-51.9	C	11.52
GGTmAmA	68.0	40.6	178.9	-113.7	-148.3	D	11.57
GGTAmG	66.1	37.8	169.8	126.0	-64.3	D	11.58
GmGTmAT	71.0	-84.6	-178.0	-112.7	-161.7	D	11.60
AmGTmAmG	145.0	-51.5	-179.3	-108.9	-83.8	D	11.72
GmGTAmG	67.8	-87.1	170.5	130.3	-66.4	D	12.06
GGTmAG	73.2	46.3	-175.1	-125.4	66.5	D	12.13
AmGmATT	128.4	-73.9	-107.8	178.8	174.8	C	12.16
GGATG	48.1	36.8	100.5	-177.1	49.5	C	12.19
AGATmG	119.4	46.3	130.3	171.2	-56.7	C	12.30
AGTmAG	144.8	87.5	-173.6	-125.1	63.3	D	12.36
GmAATG	78.5	-96.5	131.4	166.7	59.4	C	12.76
AmGTmAmA	147.0	-42.0	-179.6	-110.1	-149.8	D	12.89
AAmATG	144.7	90.6	-133.2	-168.4	58.0	C	13.28
AmGTmAG	145.9	-38.8	-171.3	-125.8	66.8	D	14.00
AAmATmG	135.5	93.7	-125.4	-171.3	-49.8	C	14.35
TGmATT	151.3	89.0	-131.3	-170.6	-161.3	C	15.44
TmAATT	150.7	-110.2	126.6	171.9	-176.9	C	15.53
GGAGG	59.2	46.5	128.2	40.5	72.3	E	17.59
GGGAG	55.0	61.7	48.6	114.9	74.4	F	18.76
GTGAG	54.7	154.2	56.0	114.7	84.5	G	60.22

^a $E = -1075852.61$ kcal/mol.

As in the case for **1**, the $-sc$ orientation around the C1–O1 bond (Φ) has not been considered in the selection of the starting structures. However, all three staggered orientations of the Ψ_1 and Ψ_4 dihedral angles have been assumed. Using this approach, 47 starting structures were generated. Optimization of the geometry led to 43 final structures. The relative energies and geometrical parameters of the relevant HF/6-31G* minima are summarized in Table 4. The relative energies of all the conformers except one are distributed in an interval of 19 kcal/mol.

The structural analysis of the 43 minima revealed that they could be grouped into seven different patterns of Mg²⁺...O coordination classified as A–G in Table 4. Each of the seven arrangements shown in Figure 3 displays a particular conformation around the P–O–P segment (Ψ_2 , Ψ_3). Four groups, namely A, E, F, and G, consist only of one conformer. Minima listed in Table 4 are characterized by the coordination of Mg²⁺ with three oxygen atoms. Exceptions are minima belonging to the group B where four oxygen atoms coordinate Mg²⁺. Surprisingly, interactions with the ring oxygen are preferred over those with the phosphoryl oxygen atoms. Since the arrangements

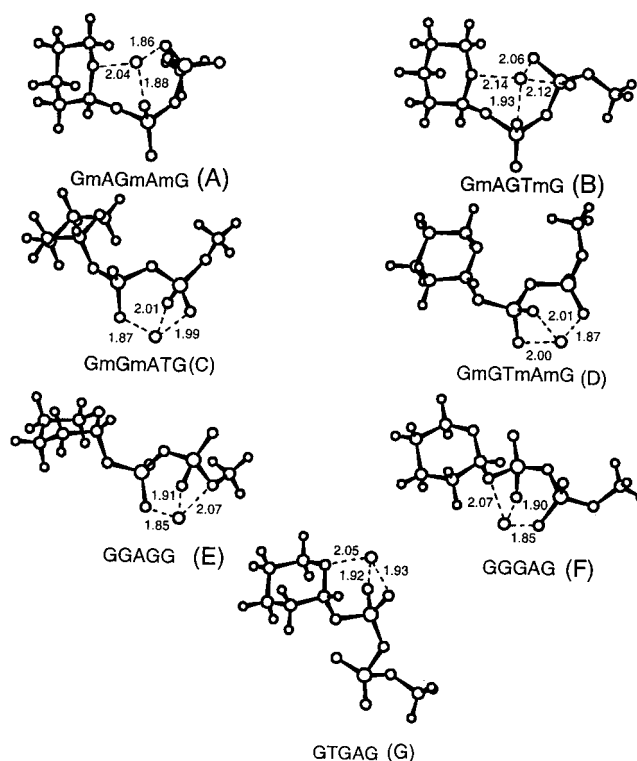


Figure 3. Representation of the seven Mg²⁺ coordination patterns visible in the structures of the magnesium 2-*O*-methyldiphosphono-tetrahydropyran complex (**2**) calculated at HF/6-31G* level. The letter illustrates the type of coordination referred to in Table 2 and dashed lines connect magnesium with the coordinated oxygen atoms. Bond lengths are given in angstroms.

A, B, and G involve an additional oxygen atom not present in the structure of the magnesium dimethyl diphosphate, these arrangements were not observed for that model.³ The most favorable conformation around the O–P–O bonds found for the magnesium dimethyldiphosphate complex, (ac, ap), corresponds to arrangement C of **2**. This arrangement is also the lowest energy conformation that does not involve the ring oxygen atom and therefore can be more directly related to the structure of the magnesium dimethyldiphosphate complex.

The two lowest energy arrangements, A and B, are characterized by interactions of the magnesium cation with the ring oxygen atom. In the lowest energy conformer (GmAGmAmG, group A), the Mg²⁺ cation interacts with two additional oxygen atoms, one from each phosphate group, whereas three additional oxygen atoms are involved in the conformers of group B. Despite this, the relative energies of the group B conformers are 4–7 kcal/mol. The highest energy arrangement (60 kcal/mol), the group G, also involves interactions of the Mg²⁺ cation with the ring oxygen atom, but in this case the coordination of the metal is with two oxygen atoms from the same nearest phosphate group. This conformation, however, exhibits a very unfavorable orientation of the phosphate group with respect to the pyranose ring. For groups C and D, three phosphoryl oxygen atoms coordinate the magnesium cation. A survey of all the minima of **2** reveals that the C–H...O hydrogen-bond interactions, such as those observed in the anionic form, are not preserved in the presence of a counterion. Only a few very weak CH...O hydrogen-bond interactions can be seen in arrangements where the metal coordination involves interactions with the ring oxygen atom such as in patterns A, B, and G. In the metal complex, interactions of the different oxygen atoms with the counterion clearly dominate over hydrogen-bonding interactions.

TABLE 5: Comparison of the ab Initio Relative Energies (kcal/mol) of Selected Magnesium 2-*O*-Methyldiphosphono-tetrahydropyran Complex (2) Conformers Calculated by Different Methods

	energy	geometry	GmAGmAmG	GmAGTmG	GGmGTG	GmGmATG	GmGTmAmG
HF	6-31G*	6-31G*	0.00	4.13	4.92	9.67	9.81
HF	6-31++G**	6-31G*	0.00	5.00	5.75	9.48	9.97
HF	6-31++G**	6-31++G**	0.00	5.06	5.73	9.33	9.93
DFT/B3LYP	6-31G**	6-31G**	0.00	2.13	3.58	12.56	12.04
DFT/B3LYP	6-31++G**	6-31G**	0.00	3.67	4.17	11.62	11.38
DFT/B3LYP	6-31++G**	6-31++G**	0.00	3.55	4.08	11.21	11.38
LMP2	6-31++G**	6-31G**	0.00	2.76	4.98	11.92	12.30
LMP2	6-31++G**	6-31++G**	0.00	2.12	3.75	10.15	10.70

TABLE 6: Summary of the Corrections to the Calculated Free Energy Differences (ZPE , $\Delta G_{\text{vibrrot}}$, $\Delta G(\text{cyclohexane})_{\text{Solv}}$, $\Delta G(\text{water})_{\text{Solv}}$), Energies (ΔE), and Estimated Free Energies (ΔG_{gas} , $\Delta G_{\text{cyclohexane}}$, ΔG_{water})^a for the Selected Magnesium 2-*O*-Methyldiphosphono-tetrahydropyran Complex (2) Conformers in the Gas Phase, Cyclohexane, and Water at 298 K (kcal/mol)

	methods	GmAGmAmG	GmAGTmG	GGmGTG	GmGmATG	GmGTmAmG
ZPE	HF/6-31G*	127.36	128.64	130.01	127.07	126.92
$\Delta G_{\text{vibrrot}}$	HF/6-31G*	-26.30	-26.56	-24.99	-27.82	-27.63
$\Delta G(\text{cyclohexane})_{\text{Solv}}$	DFT/B3LYP/6-31G**	-18.64	-14.82	-16.08	-22.62	-22.82
$\Delta G(\text{water})_{\text{Solv}}$	DFT/B3LYP/6-31G**	-63.59	-48.80	-59.80	-76.24	-66.84
ΔE	HF/6-31++G**	0.00	5.06	5.73	9.33	9.93
ΔG_{gas}		0.00	4.57	8.03	9.58	9.59
$\Delta G_{\text{cyclohexane}}$		0.00	8.39	10.59	5.40	5.41
ΔG_{water}		3.28	22.63	15.10	0.00	9.62
ΔE	DFT/B3LYP/6-31++G**	0.00	3.55	4.08	11.21	11.38
ΔG_{gas}		0.00	4.57	8.04	9.40	9.61
$\Delta G_{\text{cyclohexane}}$		0.00	8.40	10.60	5.42	5.43
ΔG_{water}		3.26	22.62	15.08	0.00	9.62
ΔE	LMP2/6-31++G**	0.00	2.12	3.75	10.15	10.70
ΔG_{gas}		0.00	3.14	7.71	8.34	8.93
$\Delta G_{\text{cyclohexane}}$		0.00	6.96	10.27	4.36	4.75
ΔG_{water}		4.31	22.24	15.81	0.00	10.00

$$^a \Delta G_{\text{gas}} = \Delta E + ZPE + \Delta G_{\text{vibrrot}}; \Delta G_{\text{cyclohexane}} = \Delta G_{\text{gas}} + \Delta G(\text{cyclohexane})_{\text{Solv}}; \Delta G_{\text{water}} = \Delta G_{\text{gas}} + \Delta G(\text{water})_{\text{Solv}}$$

Calculated geometrical parameters for five conformers of **2** are listed in Table S2 of the Supporting Information. Comparison of these data revealed that in the case of **2**, the influence of the basis set on the conformer geometry is smaller compared to that calculated for **1**. For example, the inclusion of diffuse functions into the basis set of the HF or DFT/B3LYP methods does not alter the bond length values. Similarly, variations of bond angles and torsional angles are rather small and do not exceed 2° and 5°, respectively. Electron correlation effects, treated by means of DFT/B3LYP, result mainly in the lengthening of the C–O and P–O bonds by 0.02–0.04 Å. The coordination pattern and the location of the representative minima remain the same. The comparable relative energy resulting from single point calculations of the different conformers also implies a similarity in the structures calculated using different basis sets and the HF and DFT/B3LYP methods. However, the relative energy of the conformers appears to be influenced by the electron correlation effects. Using the LMP2/6-31++G** results as a benchmark, it is evident that the relative energy of the GmAGTmG and GGmGTG conformers decreases by 2–3 kcal/mol compared to the HF/6-31++G** results (Table 5). These two structures are more compact than the three other conformers given in Table 5 suggesting that dispersion interactions are not adequately described in these complexes at the HF level.

A number of different contributions to the free energy of each conformer in the gas phase and in two solvents are given in Table 6. It is clear that their influence on the conformational equilibrium for **2** is more pronounced than in the case of **1**. Thermodynamic contributions stabilize the GmAGmAmG, GmGmATG, and GmGTmAmG conformers up to 6 kcal/mol. Though the absolute magnitudes of solvation energies are

smaller, compared to those of **1**, they show a surprisingly large variability with differing conformations. In cyclohexane, the solvation energy varies by 8 kcal/mol and in water as much as 28 kcal/mol. As a consequence, the conformational preference is shifted from GmAGmAmG in the gas phase and cyclohexane to the GmGmATG conformer in water. Unfortunately no experimental data are available for a comparison. However, because the same approach correctly predicts the p*K*_a values for a large set of different molecules,⁸ we expect the solvation energies to be reasonably well predicted.

The interaction energy of a cation with the first shell of ligands is stronger than water–water or ligand–ligand interactions.²¹ As a result, the first coordination shell of a cation in aqueous solution is well-defined and metal cations may possibly have a full coordination shell. The most common first coordination shell of Mg²⁺ is a six-coordinated octahedron and the energetics of the interactions of Mg²⁺ with water, formamide, and formate ligands has been studied using ab initio methods.^{22,23} From the coordination patterns observed for **2** (Table 4), it is clear that the oxygen atoms of the 2-*O*-methyldiphosphono-tetrahydropyran dianion (**1**) interacting with Mg²⁺ only occupy a fraction of the binding sites accessible in the first coordination shell of the metal. Assuming an octahedral geometry for the Mg²⁺, two to three binding sites are not occupied in the different conformers of **2**. To evaluate the effect of the first coordination shell of Mg²⁺ on the stability of **2**, calculations were performed on several conformers of **2** in which the first coordination shell was saturated by the addition of water molecules. Though the size and the polarity of a ligand determines the magnitude of metal–ligand interactions,²³ we restricted the binding ligands to water molecules. On the basis of the diphosphate–Mg²⁺ coordination patterns described in Table 4, we have selected

TABLE 7: Ab Initio Relative Energy (kcal/mol), Binding Energy Per One Water Molecule (kcal/mol), and the Position of the Magnesium 2-*O*-Methyldiphosphono-tetrahydropyran Complex (2) Conformers in Clusters with N_{water} Water Molecules at the HF/6-31G* Level

starting conformers	cluster conformation	Φ	Ψ_1	Ψ_2	Ψ_3	Ψ_4	ΔE	BE ^a
		Two Water Molecules ($N_{\text{waters}} = 2$)						
GGmGTG	GGmGTG	52.5	62.4	-93.1	-177.1	58.9	0.00 ^b	30.6
		Three Water Molecules ($N_{\text{waters}} = 3$)						
GmAGmAmG, GmAGTmG	GmAGmAmG	84.9	-133.3	87.3	-149.7	-67.0	0.00 ^c	29.2
ATATmG	AmAGTmG	93.8	-141.5	96.6	-171.1	-54.9	2.78	32.0
GmGmATG	GmGmATG	77.4	-82.1	-97.0	171.6	53.4	6.59	30.3
GmGTmAmG	GmGTmAmG	70.7	-80.9	172.5	-91.4	-68.2	6.68	30.3
		Four Water Molecules ($N_{\text{waters}} = 4$)						
GGAGG	GGAGG	57.7	-80.5	171.8	68.6	66.4	0.00 ^d	30.0
GGGAG	GGGAG	172.5	107.1	60.9	113.4	76.6	3.20	29.5
GTGAG	GTGAG	57.1	174.9	70.8	97.8	80.9	33.26	32.4

^a BE is a crude estimate of the binding energy for a single water calculated as $BE = -[E(\text{cluster}) - E(2) - N_{\text{water}}E(\text{water})]/N_{\text{water}}$ with $E(\text{water}) = -47\,697.56$ kcal/mol. ^b $E = -1\,171\,303.99$ kcal/mol. ^c $E = -1\,219\,032.65$ kcal/mol. ^d $E = -1\,266\,745.00$ kcal/mol.

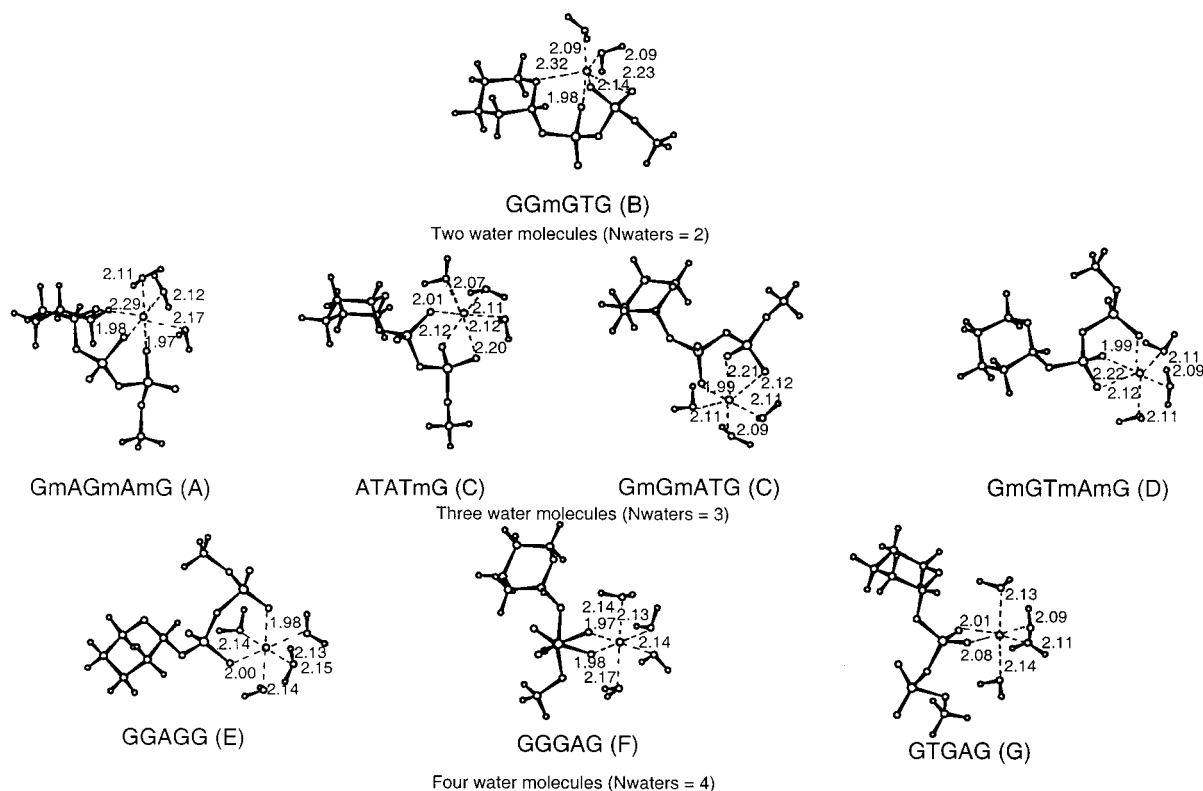


Figure 4. Representation of the eight clusters of the magnesium 2-*O*-methyldiphosphono-tetrahydropyran complex (2) with full first coordination shell of the metal calculated at HF/6-31G* level. Dashed lines connect magnesium with the coordinated oxygen atoms. Bond lengths are given in angstroms.

nine representative conformers, namely GmAGmAmG (group A), GmAGTmG (group B), GGmGTG (group B), GmGmATG (group C), GmGTmAmG (group D), ATATmG (group C), GGAGG (group E), GGGAG (group F), and GTGAG (group G). The first coordination shell was filled out by two, three, or four water molecules, and these clusters were optimized at the HF/6-31G* level. The starting geometry for the clusters was based on the HF/6-31G* optimized structure of a given conformer with the oxygen atoms of the water molecules placed in the unoccupied sites of an octahedron. The results are summarized in Table 7 and the optimized structures are shown in Figure 4. Comparison of data given in Tables 4 and 7 shows clearly that the orientations about the sugar–diphosphate linkages in the clusters are changed compared to those observed for 2 when the Mg^{2+} coordination is incomplete. The difference in some dihedral angles can be as large as 60°. These adjustments somehow allow the given cluster to adopt the best

possible octahedral symmetry and thus maximize the binding. The clusters do not possess an ideal octahedral symmetry due to the different nature of the ligands and to some conformational constraints of the sugar–diphosphate linkages. Nevertheless, all clusters examined present four oxygen atoms (two from water molecules and two from 2) in nearly the same plane as the Mg^{2+} ion. This arrangement reduces the ligand–ligand repulsive interactions. The distance between the metal and water oxygens varies from 2.0 to 2.2 Å. From the data in Table 7, it can be seen that the estimated binding energies are roughly in the range of 29–33 kcal/mol. We have not attempted to evaluate more accurately the binding energies because this is not the primary aim of this paper and it would require extensive calculations of several other contributions.²³ The saturation of the unoccupied octahedral sites by water molecules results in a decrease in the relative energy of the conformers. These results imply that a magnesium complex with the pyrophosphate functional group

in nucleotide–sugars may adopt different conformations depending on the structural features imposed by the arrangement of the ligands in the first coordination shell of the metal.

4. Conclusions

The goal of this study was to describe the conformational properties of the sugar–diphosphate linkage in different environments. The results of the conformational analyses of **1** and **2** clearly show that interactions of the diphosphate group with the Mg^{2+} cation alter the conformational preferences around the diphosphate linkage. In the absence of a metal counterion, the (Ψ_2 , Ψ_3) torsion angles clearly prefer the (sc, ac) or (–sc, –ac) orientations but complexation by a metal cation changes this preference to (sc, –ac). As has already been observed for sodium 2-*O*-methylphosphono-tetrahydropyran, complexation with a metal counterion also changes the conformation about the anomeric C1–O1 linkage from the ac to sc orientation. The Ψ_1 dihedral angle does not remain inert to the effects of the complexation either. This demonstrates that interactions with a metal counterion induce some conformational changes in diphosphate linkages. These changes influence the overall 3D shape adopted by nucleotide–sugars and therefore might have consequences for their functions in biological processes. They also suggest that for an accurate overall description of the conformational behavior of those compounds, a reliable estimate of thermodynamic and solvent contributions should be included in the calculations. Finally, inclusion of water molecules to complete the first solvation shell of the Mg^{2+} ion had significant effects on the preferred conformations of the complex. The results of this study indicate that a delicate balance between intramolecular and intermolecular interactions determines the conformational equilibrium around the sugar–diphosphate linkages; as a result, several different conformations can be adopted, depending on the environment. In particular, when complexed with a protein, the conformation could be significantly affected depending on the nature and geometry of the specific ligands provided by the protein-binding site.

Supporting Information Available: Tables of relevant bond lengths, bond angles, and torsional angles for the five selected conformers of the 2-*O*-methylidiphosphono-tetrahydropyran di-

anion (**1**) and the magnesium 2-*O*-methylidiphosphono-tetrahydropyran (**2**) calculated by different ab initio methods. This material is available free of charge via Internet at <http://pubs.acs.org>.

References and Notes

- (1) Schachter, H. *Curr. Opin. Struct. Biol.* **1991**, *1*, 755–765.
- (2) Dennis, J. W.; Laferte, S.; Waghome, C.; Breitman, M. L.; Kerbel, R. S. *Science* **1987**, *236*, 582–585.
- (3) Tvaroska, I.; André, I.; Carver, J. P. *J. Mol. Struct. (THEOCHEM)* **1999**, *469*, 103–114.
- (4) Tvaroska, I.; André, I.; Carver, J. P. *J. Phys. Chem. B* **1999**, *103*, 13, 2560–2569.
- (5) Wang, R.; Steensma, D. H.; Takaoka, Y.; Yun, J. W.; Kajimoto, T.; Wong, C.-H. *Bioorg. Med. Chem.* **1997**, *5*, 661–672.
- (6) Turbomole 95.0 User Guide, version 2.3.5; San Diego: Biosym/MSI, 1995.
- (7) Schmidt, M. S.; Baldrige, K. K.; Boatz, J. A.; Elbert, S. T.; Gordon, M. S.; Jensen, J. H.; Koseki, S.; Matsunaga, N.; Nguyen, K. A.; Su, S. J.; Windus, T. L.; Dupuis, M.; Montgomery, J. A. *J. Comput. Chem.* **1993**, *14*, 1347–1363.
- (8) Jaguar 3.5, Schrödinger, Inc., Portland, OR, 1998.
- (9) Becke, A. D. *J. Chem. Phys.* **1993**, *98*, 5648–5652.
- (10) Parr, R. G.; Yang, W. *Density-Functional Theory of Atoms and Molecules*; Oxford University Press: New York, 1989.
- (11) Murphy, R. B.; Beachy, M. D.; Friesner, R. A.; Ringnalda, M. N. *J. Chem. Phys.* **1995**, *103*, 1481–1490.
- (12) Tannor, D. J.; Marten, B.; Murphy, R.; Friesner, R. A.; Sitkoff, D.; Nicholls, A.; Ringnalda, M.; Goddard, W. A., III; Honig, B. *J. Am. Chem. Soc.* **1994**, *116*, 11875–11882.
- (13) Tvaroska, I.; Carver, J. P. *J. Phys. Chem.* **1996**, *100*, 11305–11313.
- (14) Steiner, T.; Saenger, W. *J. Am. Chem. Soc.* **1992**, *114*, 10146–10154.
- (15) Desiraju, G. R. *Acc. Chem. Res.* **1991**, *24*, 290–296.
- (16) Aakeroy, C. B.; Seddon, K. R. *Chem. Soc. Rev.* **1993**, 397–407.
- (17) Schneider, B.; Kabelac, M.; Hobza, P. *J. Am. Chem. Soc.* **1996**, *118*, 12207–12217.
- (18) Saint-Martin, H.; Ruiz-Vicent, L. E.; Ramirez-Solis, A.; Ortega-Blake, I. *J. Am. Chem. Soc.* **1996**, *118*, 12167–12173.
- (19) Tvaroska, I.; Bleha, T. *Adv. Carbohydr. Chem. Biochem.* **1989**, *47*, 45–123.
- (20) Colvin, M. E.; Evleth, E.; Akacem, Y. *J. Am. Chem. Soc.* **1995**, *117*, 4357–4362.
- (21) Lehn, J.-M. *Structure and Bonding*; Dunitz, J. D., Hemmerich, P., Ibers, J. A., Jorgensen, C. K., Neilands, J. B., Reinin, D., Williams, R. J. P., Eds.; Springer-Verlag, Inc.: New York, 1973; Vol. 16, pp 1–69.
- (22) Deerfield, I.; D. W.; Lapadat, M. A.; Spremulli, L. L.; Hiskey, R. G.; Pedersen, L. G. *J. Biomol. Struct. Dynamics* **1989**, *6*, 1077–1091.
- (23) Krauss, M.; Stevens, W. J. *J. Am. Chem. Soc.* **1990**, *112*, 1460–1466.